APPENDIX B

THERMAL MODELING

B.1 INTRODUCTION

The thermal performance information presented in Sections 2.2, 2.3, and 2.4 of this environmental impact statement (EIS) was calculated with the aid of three models. The Cooling-Tower Performance (CTPERF) model computes effluent stream (water and air) temperatures as a function of influent stream properties and tower design. The Surface-water Heat, Savannah River Plant (SHSRP) model computes downstream temperatures along the SRP streams (Four Mile Creek, Pen Branch, Steel Creek, and Beaver Dam Creek) that receive cooling water effluent. The latter computation is performed as a function of effluent stream and extant meteorological properties. The Savannah River Dilution - D-Area (SRDD) model computes the temperature or dilution distribution in the Savannah River from D-Area based on discharge design and river flow.

In addition to a discussion of these three thermal performance models, this appendix also provides a brief description of the model (FOG) that has been used to calculate cooling system fogging, icing, visible plumes, and drift deposition.

B.2 COOLING-TOWER PERFORMANCE MODEL (CTPERF)

B.2.1 MODEL DESCRIPTION

The cooling of artificially heated water, such as the heated secondary cooling water at C- and K-Reactors, is a surface transport phenomenon between the water and the heat receptor (in this case the atmosphere). The cooling towers described in Chapter 2 of this EIS are efficient in this heat transfer because they maximize the exposed surface area of the water (via droplet formation) and introduce a heat sink (air) that does not contain residual heat from tower operation (due to the buoyancy of the heated air stream).

The heat-transfer process involves, chiefly, the transfer of latent heat due to the evaporation of a small portion of the water; a secondary cooling process is the transfer of heat due to the temperature difference between air and water. The theoretical limit to which the influent water temperature can be cooled is determined by the temperature and moisture content of the influent air stream. The wet-bulb temperature (t_{wb}), which is the temperature of saturated air at the same enthalpy (heat content) as the influent air, is an indication of the temperature and moisture content of the influent air and, as such, represents the theoretical limit to which the influent water temperature can be cooled. Practically, the cold-water temperature approaches, but does not equal, the wet-bulb temperature. The closeness of the approach depends on tower design parameters such as air-water contact time and droplet size (Perry, 1963).

The present analysis is based on the generally accepted Merkel equation (Perry, 1963).

$$\frac{KaV}{L} = \int_{t_2}^{t_1} \frac{dt}{h' - h} \tag{1}$$

where K = mass transfer coefficient, $gm/hr/m^2$
a = contact area, m^2/m^3 of tower volume
V = active cooling volume, m^3
L = water flow rate, gm/hr
h' = enthalpy of saturated air at the water temperature, cal/gm
h = enthalpy of influent air stream, cal/gm
t_1 = temperature of influent water stream, °C
t_2 = temperature of effluent water stream, °C

Equation 1 expresses the mechanism of each droplet of water being surrounded by a film of air and the enthalpy difference between the film and surrounding air providing the driving force for the heat transfer. The left-hand side of Equation 1 is entirely in terms of tower-operating parameters, while the right-hand side is entirely in terms of air and water properties.

The latter characteristic of Equation 1 facilitates its use to compute tower performance. Tower design conditions (t_1, t_2, and t_{wb}) completely specify the value of the integral on the right-hand side of Equation 1. This value, called the tower characteristic, is dependent only on tower design parameters. Accordingly, t_2 can be obtained by implicitly solving Equation 1 for any given air wet-bulb temperature (t_{wb}), which defines h, hot-water temperature (t_1), and tower characteristic (determined, as described above, from design conditions). In addition, effluent air temperature is calculated by a heat balance approach; that is, the heat lost by the water in the tower is equated to the heat gained by the air.

As discussed above, the enthalpy difference h'-h is the driving force for cooling. The larger this difference, the more rapid the cooling of the water. Mathematically, the right-hand side of Equation 1 is the area under the $\frac{1}{h' - h}$ vs. t curve from t_2 to t_1.

At large values of t (i.e., close to t_1), the fraction $\frac{1}{h'-h}$ is very small.

As t decreases, the fraction correspondingly increases until, at $t = t_{wb}$, the fraction becomes infinite (the theoretical limit of cooling). This behavior of the integral can be related to the left-hand side of Equation 1, which indicates (for given flow rates) the tower characteristics. The cooling of the water from its initially high temperatures is very rapid and uses a small fraction of the tower. The cooling of the water at low temperatures is very slow and uses the major part of the tower. In terms of tower design, the size of the tower increases (approximately) exponentially for each increment of cooling desired.

The air flow rate is specified (constant) for the fan-driven mechanical draft tower. For the natural draft tower, the air flow rate is a function of the density difference between the incoming and outgoing air. The dry air flow rate can be derived by applying the Bernoulli equation and continuity to the tower inlet and outlet cross-sections. The result is:

$$G = A_2 U_2 \left(\frac{\rho_1}{1 + H_1}\right)$$

where: $$U_2^2 = \frac{2 g_c y \left(\frac{\rho_1 - \rho_2}{\rho_2}\right)}{1 + k \frac{\rho_2}{\rho_1}\left(\frac{A_2}{A_1}\right)^2}$$ BB-3 BC-4 BC-14 BC-15

g_c = 980 dynes/gm
y = tower height, m
ρ = density of air, gm/m^3
k = loss coefficient
A = cross-section area, m^2
U = air velocity, m/sec
H = absolute humidity, gm-water/gm-dry air
G = dry air flow rate, gm/sec
subscript 1 = tower inlet
subscript 2 = tower outlet

CTPERF model results have shown excellent comparison with published tower design curves (Dickey and Cates, 1973).

B.2.2 MODEL USE

Table B-1 contains mean and maximum monthly wet bulb temperatures for the period 1952-1982 (Morris, 1987a). Tower effluent water temperatures, also given in Table B-1, are based on vendor supplied information. CTPERF was used to calculate performance equations relating effluent air temperatures and flow rates as a function of influent air wet bulb temperature and relative humidity. BB-3 BC-4

Once-through tower influent water temperatures, T_1, were based on monthly average reactor intake (Savannah River) temperatures (DOE, 1984a). These reactor intake temperatures were elevated by the temperature rise through the reactor heat exchangers, which can be described (Neill and Babcock, 1971; NUS Corporation, 1984) as

$$\Delta T = 65.79 - .6568\, T_{in} \qquad (2)$$

where ΔT = maximum reactor power secondary cooling water temperature rise across reactor heat exchangers, °C
T_{in} = reactor intake temperature, °C

Adding T_{in} to Equation 2 yields

$$T_1 = 65.79 + .3433\, T_{in} \qquad (3)$$

Table B-1. Monthly Average and Maximum Cooling-Tower Temperatures (°C)

Temperature	Jan	Feb	Mar	Apr	May	June	July	Aug	Sept	Oct	Nov	Dec
Wet-bulb temperature												
Monthly average[a]	4	6	11	14	18	22	23	23	21	14	10	6
Monthly maximum[b]	20	20	21	24	25	26	27	27	26	25	23	21
Savannah River temperature												
Monthly average	8	8	11	15	18	21	23	23	22	19	15	11
Once-through tower effluent temperature												
Monthly average	19	20	23	24	26	28	29	29	28	24	23	21
Monthly maximum	28	28	28	30	30	31	32	32	31	31	29	28
Recirculating tower effluent temperature												
Monthly average	14	15	18	20	23	26	27	26	25	20	18	15
Monthly maximum	25	25	26	28	28	29	30	30	29	28	27	26

[a]Based on average dry bulb temperature and relative humidity.
[b]Based on maximum monthly dry bulb and coincident relative humidity.

BB-3
BC-14
BC-15

Recirculating influent water temperatures are determined by imposing Equation 3 on the tower performance calculations. That is, rather than specifying the influent tower water temperature, T_1, and calculating the effluent water temperature, T_2, the calculation imposes the functional relationship

$$T_1 = 65.79 + .3433T_2 \quad (4)$$

onto the implicit cooling-tower calculations. Effluent natural draft water temperatures were used as influent water temperatures for the mechanical draft tower in the recirculating system. BB-3 BC-4

B.2.3 MODEL RESULTS

The above information was used to calculate the effluent air performance equations for once-through (design conditions: T_2 = 32.2°C, T_{wb} = 27.8°C) and recirculating (natural draft design conditions: T_2 = 38.1°C, T_{wb} = 26.7°C; mechanical draft design conditions: T_1 = 38.1°C, T_2 = 29.4°C, T_{wb} = 26.7°C) towers (Morris, 1987a). These results were used in simulating environmental effects (fogging, icing, aesthetics, deposition) from the effluent air stream (see Section B.5). Table B-1 includes the mean and maximum monthly effluent water temperature for each system type. The effluent water temperatures listed in Table B-1 are those included in the Chapter 2 thermal performance analyses. BB-3 BC-4

The once-through towers are designed to meet State Class B water classification standards of a maximum instream temperature of 32.2°C at the point of discharge to the creeks. Table B-1 shows that the tower discharge will meet this requirement for all monthly maximum conditions. BC-14 BC-15

The recirculating towers are also designed to meet State Class B water classification standards. However, because the effluent water also serves as influent water, this system has been designed to further lower the water temperature. A comparison of once-through and recirculating tower effluent temperatures in Table B-1 illustrates this difference.

B.3 SURFACE-WATER HEAT, SAVANNAH RIVER PLANT MODEL (SHSRP)

B.3.1 MODEL DESCRIPTION

As in the case of CTPERF, the cooling of artificially heated surface waters is a transport phenomenon between the water and the heat receptor (the atmosphere). Unlike the cooling towers, however, other processes contribute to this heat transfer.

The flux of heat across the water surface has various components that can be either positive (heat entering the water) or negative (heat exiting the water). The major processes are solar radiation, atmospheric radiation, back radiation from the water body, evaporation, and conduction.

The net solar heat flux, ϕ_{sn}, consists of incident solar radiation minus reflected solar radiation. The incident, clear-sky, solar radiation is a function of latitude, time of day, and time of year. In addition, reflection, scattering, and absorption by gases, water vapor, and particulates in the atmosphere will affect this term. Accordingly, empirical representations are usually used to calculate the temporal distribution of incident solar radiation at a particular site. Reflected solar radiation from the water surface ranges from 5 to 10 percent of incident radiation (Thackston and Parker, 1971). A value of 6 percent was used in producing the baseline data for this study. The reduction of incident solar radiation by cloud cover is described by the factor $(1 - .65c^2)$ where c is the cloud cover (range of 0 to 1). The net temporal distribution of solar radiation used as the baseline for this study was produced by the UHSPOND code (Codell and Nuttle, 1980). The back radiation from the water surface is essentially "black body" radiation. The latter is described by the Stephan-Boltzmann law (Bird, Stewart, and Lightfoot, 1966):

$$\phi_b = \varepsilon\sigma(T_s + 273)^4 \tag{5}$$

TE

where ε = atmospheric emissivity (1 for a theoretical black body)
σ = Stephan-Boltzmann constant (1.17×10^{-6} Cal/m^2 - day - $^\circ$K)
$T_s + 273$ = absolute temperature of the water surface in $^\circ$K

The emissivity of the water is well-known as 0.97 (Ryan and Stolzenbach, 1972). The long-wave atmospheric radiation, ϕ_a, is also described by Equation 5, except that the temperature used is that of the atmosphere, T_a. The emissivity of the atmosphere can be empirically described as

$$\varepsilon = 9.4 \times 10^{-6}\ (T_a + 273)^2\ (1 + .17c^2) \tag{6}$$

where the cloud-cover term describes the darkening of the sky and the attendant increase in emissivity. The net atmospheric radiation, ϕ_{an}, is taken as 97 percent (the water surface reflecting 3 percent) of the incident radiation (Ryan and Stolzenbach, 1972).

The evaporative heat flux, ϕ_e, from the water surface is mechanically equivalent to the latent heat of vaporization of the water being evaporated into an atmospheric boundary layer (which is in equilibrium with the water surface) and subsequently transported to the atmosphere. This transport (convection) of heat has two components: forced convection (due to the wind) and free convection (due to buoyancy effects).

The forced convection term, ϕ_{e1}, is empirically described as

$$\phi_{e1} = kW_2\ (e_s - e_a) \tag{7}$$

TE

where k = a constant
W_2 = the wind speed 2 meters above the water surface in meters per second
e_s = the saturated vapor pressure at the temperature of the water surface in mm Hg
e_a = the vapor pressure of the air (mm Hg)

The form of the free convection term, ϕ_{e2}, is taken from experimental work of free convection over a flat plate modified by the fact that water vapor is lighter than air (and, therefore, evaporation increases the buoyancy forces) (Ryan and Stolzenbach, 1972). The result is

$$\phi_{e2} = 18.4\ (T_{sv} - T_{av})^{1/3}\ (e_s - e_a) \qquad (8)$$

TE

where $T_v = (T + 273)/(1 - .378e/p)$
$e = e_a$ and $T = T_a$ for $T_v = T_{av}$
$e = e_s$ and $T = T_s$ for $T_v = T_{sv}$
p = atmospheric pressure in mm Hg

The total evaporative heat flux, ϕ_e, is then the sum of $\phi_{e1} + \phi_{e2}$. A value of $k = 31.3$ (for the units given above) has been found to be appropriate (Ryan and Stolzenbach, 1972).

Previous studies have shown that the evaporative heat flux as calculated by Equations 7 and 8 is too large. A multiplicative constant, C, can be defined that results in a better approximation to the actual flux. A value of 0.78 has been found elsewhere (Firstenberg and Fisher, 1976) and is used here.

Heat conducted from the water to the atmosphere via the atmospheric boundary layer must be transported analogously to the convection of evaporative heat flux. The heat conduction flux, ϕ_c, is related to ϕ_e through the Bowen Ratio; that is

$$\phi_c/\phi_e = R(T_s - T_a)/(e_s - e_a) \qquad (9)$$

where R = .46 mm Hg/°C (Ryan and Stolzenbach, 1972).

The total heat flux, ϕ, into the water surface is then:

$$\phi = \phi_{sn} + \phi_{an} - \phi_b - \phi_e - \phi_c \qquad (10)$$

Equation 10 allows the total heat flux to be calculated, given the solar radiation, air temperature, cloud cover, water temperature, wind speed, and relative humidity. For a given set of meteorological conditions, the only variable in this list is the water temperature, T_s. For the site streams, where the flow will be vertically well mixed (due to turbulent and shallow flow) and plug flow in character (due to the long, narrow nature of the streams and the assumed steady flow and meteorology), the equation describing the conservation of heat can be written as (Harleman, 1972)

$$\frac{UdT}{dx} = \frac{\phi}{\rho cd} \qquad (11)$$

where U = average cross-section velocity, m/sec
T = water temperature, °C
x = downstream distance, m
ρ = density of water, gm/m^3
c = specific heat of water, cal/gm-°C

d = depth, m
ϕ = total heat flux into the water surface, cal/m^2-sec

Equation 11 quantitatively expresses that the change in heat content of the creek over a given distance (left-hand side of equation) is equal to the heat passing through the water surface over this distance (right-hand side of equation). For a given discharge and a given distance, all parameters in Equation 11 are known except for T and ϕ. Equation 11 together with Equation 10 allows the computation of T vs. x.

To facilitate the computation and illustrate the behavior of the solution, the concepts of surface-heat-exchange coefficient and equilibrium temperature are introduced. The surface-heat-exchange coefficient, K, relates the change in heat transfer rate to the change in water surface temperature (Edinger and Geyer, 1965):

TC

$$K = \frac{-\partial\phi}{\partial T} \qquad (12)$$

The equilibrium temperature, T_e, is the temperature that the water approaches for a given set of meteorological conditions (analogous to the wet-bulb temperature for cooling towers) and is that temperature at which ϕ = 0 (calculated from Equation 10). Integrating Equation 12 and noting the definition of T_e yields:

$$\phi = -K\,(T - T_e) \qquad (13)$$

which, when substituted in Equation 11, results in:

$$\frac{dT}{T-T_e} = \frac{-KW}{cQ}\,dx \qquad (14)$$

where Q = flow rate, m^3/sec
W = surface width, m
Q/W = Ud

Equation 14 can be integrated (for constants K, Q, W, and T_e) to give:

$$\frac{T_1 - T_e}{T_2 - T_e} = \exp\ \frac{KW}{\rho cQ}\,(x_2 - x_1) \qquad (15)$$

where the subscript 1 indicates the inflow location and subscript 2 indicates the outflow location.

In typical applications (e.g., steam power plants) where the heat-exchange temperature rise is relatively small (e.g., 10°C), Equation 15 can be directly applied. However, for such applications as the highly elevated discharge temperatures from the existing C- and K-Reactor systems, the value of K cannot be considered constant over the large ranges of temperature, $T_1 - T_2$. This is illustrated in Figure B-1, which shows K vs. T for typical site summer meteorological conditions. [Analogous to the cooling-tower analysis, the rate of cooling at high temperatures (high K) is much more rapid than that at low temperatures (low K) due to the exponential relationship between K and

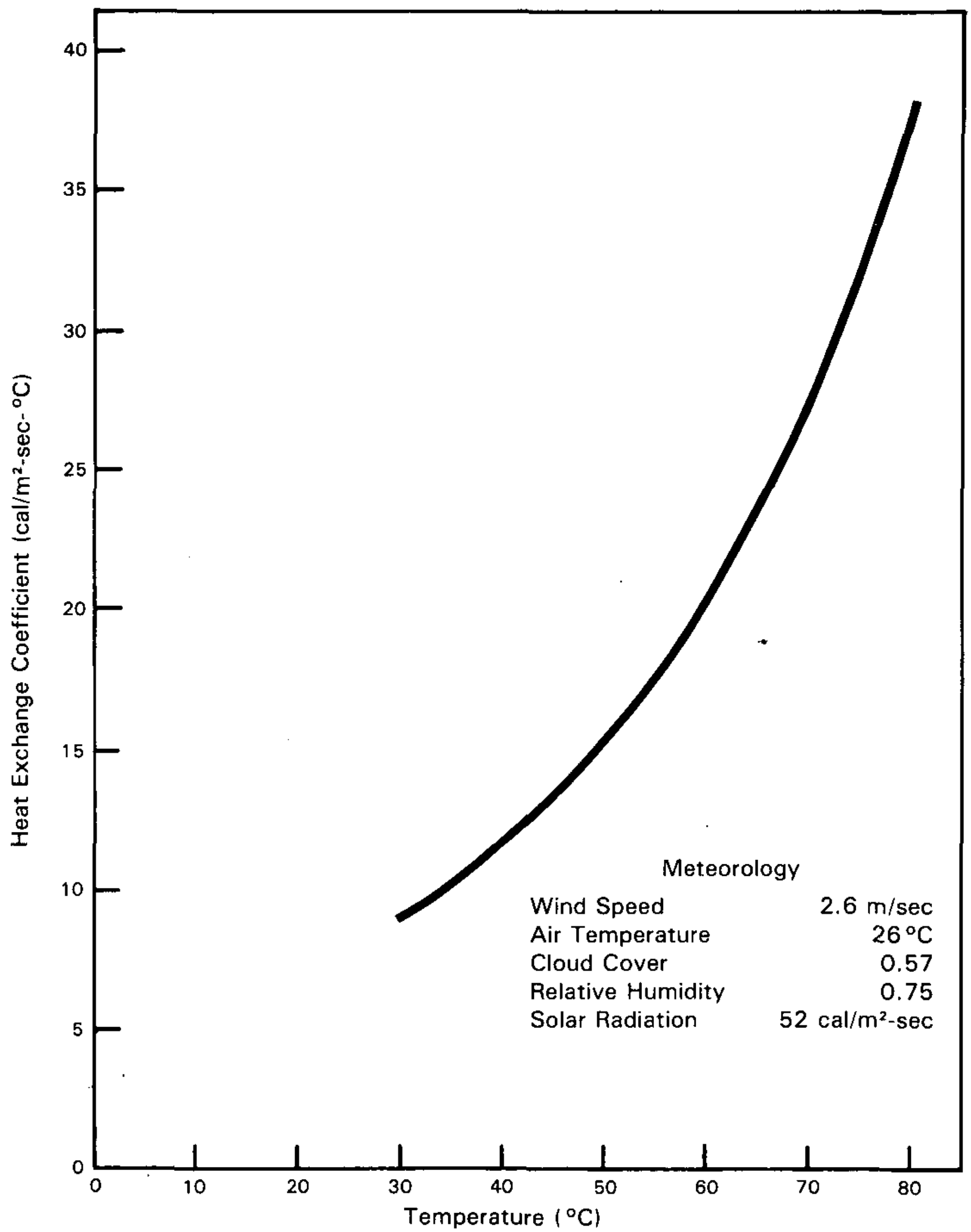

Figure B-1. Heat Exchange Coefficient vs Temperature (Typical Summer Conditions)

the water temperature]. Accordingly, SHSRP computes Equation 15 iteratively; that is, a series of small temperature steps, $T_1 - T_2$, are taken and the summation of the corresponding values of $x_2 - x_1$ is calculated. The process is repeated until the summation matches the required value.

SHSRP results have been compared with analytic solutions to the heat balance problem (Ryan, 1972). With the conditions for which analytic solutions are feasible (i.e., constant stream width), the two methodologies were in exact agreement. The results of SHSRP, with variable stream width, were also compared with temperatures measured in the thermally loaded SRP streams, Pen Branch and Four Mile Creek. Ground truth and remote sensing data for eight dates, which covered all seasons and a variety of operating modes, were used for the comparison. The Pearson product-moment correlation coefficients, which measure the linear relationship (or trend) between the measured and predicted temepratures, were found to be 0.93 and 0.86 for Pen Branch and Four Mile Creek, respectively. These coefficients indicate that SHSRP is a valuable tool in predicting SRP stream temperatures. The difference from a perfect correlation (coefficient = 1) could be explained by the error inherent in the measured temperatures, the uncertainty of the extant ambient flows, and the fact that the measurements are instantaneous, whereas the model uses daily average information.

B.3.2 MODEL USE

BC-4 BC-14 BC-15 SHSRP was used to calculate downstream temperature distributions during monthly average and extreme meteorological conditions for the various cooling-system alternatives for C- and K-Reactors and the D-Area powerhouse. Meteorological conditions (wind speed, air temperature, cloud cover, solar radiation, and relative humidity) were taken as those measured at Bush Field for the 30-year period 1953 to 1982 (NCDC, 1983). Table B-2 contains the minimum, mean, and maximum monthly average meteorological parameter values for the period of record.

BC-4 BC-14 BC-15 Equilibrium temperatures for daily average meteorological conditions were calculated for the 30-year period, and monthly averages of these values are given in Table B-2. Extreme monthly meteorological conditions were chosen as those extant during the months corresponding to the maximums in Table B-2. Average monthly meteorological conditions are the mean monthly averages given in the same table.

B.3.3 MODEL RESULTS

The above information was used to calculate the downstream temperatures in Four Mile Creek, Pen Branch, and Beaver Dam Creek during monthly average and extreme meteorological conditions. Downstream temperatures for the various alternatives and creeks, as illustrated in Figure B-2, are compiled in Tables B-3 through B-5.

BC-4 BC-14 BC-15 The tower discharge temperatures are based on the appropriate values from Table B-1. The once-through tower discharge flow rate is 11 cubic meters per second and the recirculating tower discharge (blowdown) flow rate is 0.7 cubic meter per second (Morris, 1987a). The annual average Four Mile Creek (at Road A-7) and Pen Branch (at Road B) flows, other than reactor effluent, are approximately 0.5 and 0.3 cubic meter per second, respectively, and are assumed to be at equilibrium temperature (Morris, 1987b).

Table B-2. Monthly Minimum, Mean, and Maximum Meteorological Parameters Used in the Analysis of Downstream Temperatures

Parameter	Jan	Feb	Mar	Apr	May	June	July	Aug	Sept	Oct	Nov	Dec
Wind speed, m/sec												
Minimum monthly average	2.3	2.9	3.2	2.6	2.3	2.1	2.1	2.1	1.9	1.9	2.0	2.3
Mean monthly average	3.2	3.5	3.6	3.4	2.9	2.8	2.6	2.5	2.5	2.6	2.8	3.0
Maximum monthly average	3.8	4.3	4.3	4.5	3.6	3.7	3.1	2.9	3.2	3.3	3.4	3.8
Air temperature, °C												
Minimum monthly average	2	4	7	14	19	23	24	24	20	15	9	4
Mean monthly average	7	8	12	17	21	25	26	26	23	17	12	8
Maximum monthly average	13	13	16	19	24	27	28	28	25	20	14	13
Cloud cover, fraction												
Minimum monthly average	.35	.27	.40	.36	.42	.37	.40	.32	.31	.16	.33	.46
Mean monthly average	.58	.54	.56	.50	.55	.56	.61	.54	.53	.42	.47	.54
Maximum monthly average	.73	.78	.73	.65	.77	.67	.80	.72	.71	.67	.61	.70
Solar radiation, cal/m²-sec												
Minimum monthly average	21	27	34	43	43	48	40	41	36	30	27	20
Mean monthly average	26	34	41	51	53	56	53	52	44	40	31	25
Maximum monthly average	33	44	48	57	61	65	64	63	54	49	36	28
Relative humidity, fraction												
Minimum monthly average	.59	.53	.56	.60	.63	.61	.66	.68	.71	.64	.63	.62
Mean monthly average	.71	.67	.66	.66	.71	.72	.75	.76	.77	.74	.72	.72
Maximum monthly average	.82	.76	.73	.79	.79	.80	.82	.84	.83	.83	.77	.80
Equilibrium temperature, °C												
Minimum monthly average	3	7	10	18	23	27	28	27	23	17	11	5
Mean monthly average	8	10	15	21	25	28	30	29	26	20	13	9
Maximum monthly average	14	15	18	23	28	30	31	31	28	22	16	13

BC-4
BC-14
BC-15

BC-4
BC-14
BC-15

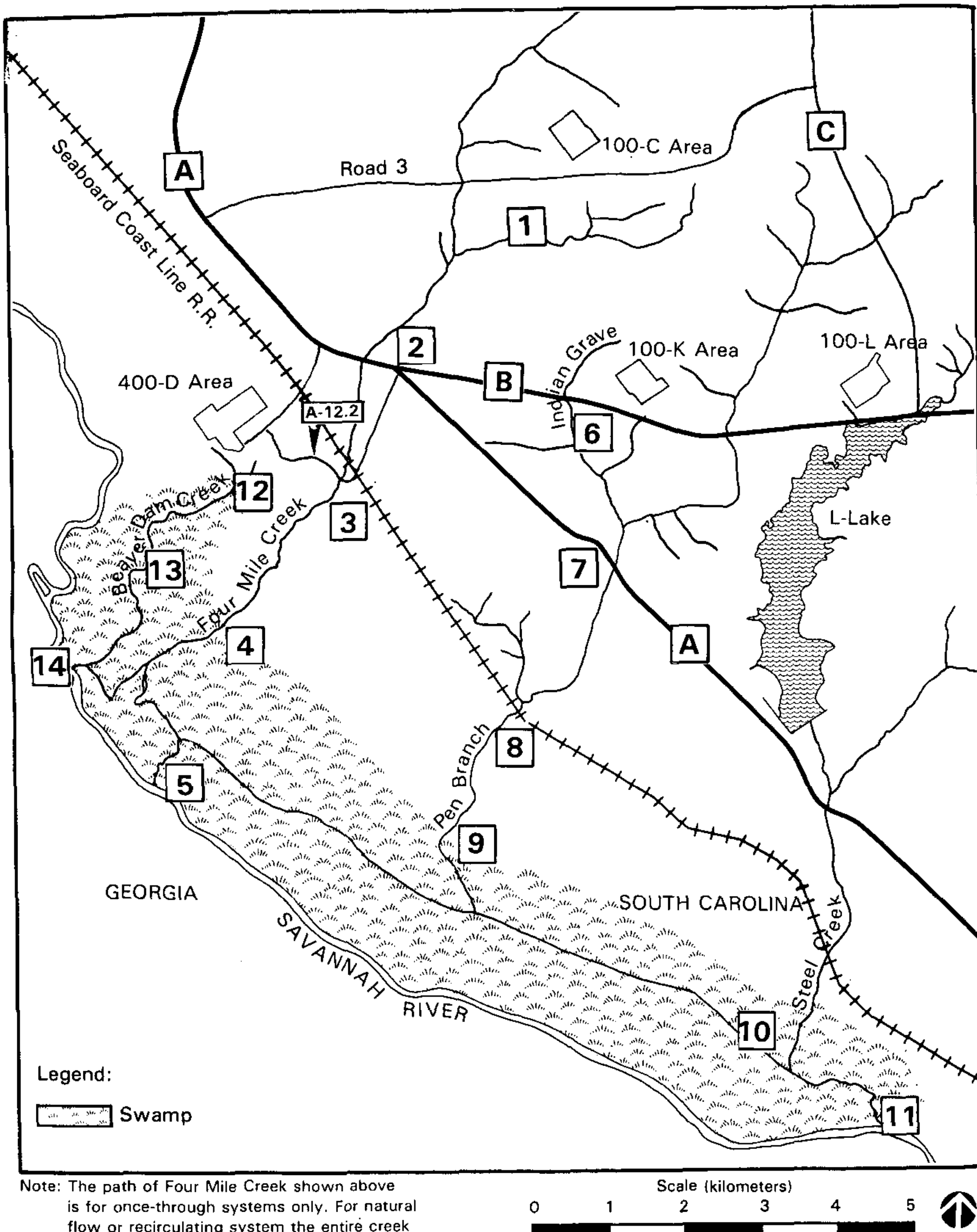

Note: The path of Four Mile Creek shown above is for once-through systems only. For natural flow or recirculating system the entire creek flow enters the Savannah River at point 5.

Scale (kilometers) 0 1 2 3 4 5

Figure B-2. Locations Corresponding to Downstream Temperatures in Tables B-3 through B-5

Table B-3. Downstream Temperature Distributions (°C) for Four Mile, Pen Branch, and Beaver Dam Creeks with Existing System[a]

Location	Month											
	Jan.	Feb.	March	April	May	June	July	Aug.	Sept.	Oct.	Nov.	Dec.
C-Reactor												
(Four Mile Creek)												
Discharge (1)[b]	69(70)	69(71)	70(72)	71(73)	72(73)	73(74)	74(75)	74(75)	73(75)	72(74)	71(73)	70(72)
Road A (2)	49(51)	49(51)	50(52)	53(55)	55(57)	57(58)	57(58)	58(58)	57(58)	55(57)	52(53)	50(52)
Road A-13 (3)	42(45)	42(44)	44(45)	46(48)	49(51)	50(51)	51(52)	51(52)	50(51)	49(50)	45(47)	43(45)
Swamp Delta (4)	32(35)	33(35)	34(36)	38(39)	40(42)	42(43)	43(43)	43(44)	42(42)	39(40)	35(37)	33(35)
Mouth (5)	24(27)	24(27)	27(29)	30(32)	33(35)	35(36)	36(37)	36(37)	34(35)	31(33)	27(29)	25(27)
Ambient Creek[c]	9(19)	11(19)	15(24)	19(25)	22(27)	25(31)	25(29)	25(29)	23(28)	21(25)	13(23)	13(18)
K-Reactor												
(Pen Branch)												
Discharge (6)	69(70)	69(71)	70(72)	71(73)	72(73)	73(74)	74(75)	74(75)	73(75)	72(74)	71(73)	70(72)
Road A (7)	61(63)	60(62)	61(63)	63(65)	66(67)	67(68)	68(69)	68(69)	68(69)	67(68)	64(66)	62(64)
RR Bridge (8)	52(54)	51(53)	52(54)	55(56)	57(59)	59(60)	59(60)	60(60)	59(60)	58(59)	54(56)	53(55)
Swamp Delta (9)	42(44)	42(44)	43(44)	46(48)	48(50)	50(51)	51(51)	51(51)	50(51)	48(49)	45(46)	43(45)
Above Steel Creek (10)	16(21)	17(21)	20(22)	24(26)	27(29)	29(30)	30(31)	30(31)	28(29)	24(26)	20(22)	17(20)
Mouth (11)	13(17)	15(18)	18(21)	21(23)	24(27)	27(28)	28(29)	28(29)	26(27)	22(24)	17(19)	14(17)
Ambient Creek[d]	8(18)	10(18)	15(22)	18(23)	21(24)	23(27)	23(27)	23(26)	21(26)	19(23)	13(21)	12(17)
D-Area												
(Beaver Dam Creek)												
Discharge (12)	18(27)	16(22)	21(27)	24(29)	28(32)	29(34)	28(33)	28(33)	27(33)	27(34)	26(33)	19(31)
Swamp Delta (13)	17(25)	16(21)	20(26)	24(28)	27(31)	28(33)	28(33)	28(32)	27(32)	26(32)	24(30)	18(28)
Mouth (14)	17(22)	17(21)	20(24)	24(27)	27(29)	29(31)	30(31)	29(31)	28(30)	25(29)	22(27)	18(23)
Ambient creek[e]	8(15)	9(14)	12(17)	15(20)	19(22)	21(25)	23(27)	23(26)	23(26)	20(23)	17(22)	12(18)

a. Temperatures are monthly average - monthly extremes are in parentheses.
b. Corresponds to stream locations shown as squares on Figure B-2.
c. U.S. Geological Survey data for water year 1985 for station 02197342; Four Mile Creek at Road A-7 (USGS, 1986).
d. U.S. Geological Survey data for water year 1985 for station 02197341; Pen Branch at Road B (USGS, 1986).
e. Average U.S. Geological Survey data for water years 1976-1985 for station 01297320; Savannah River near Jackson, S.C. (USGS; 1977, 1978, 1979, 1980, 1981, 1982, 1983, 1984, 1985, 1986).

BC-4
BC-14
BC-15

Table B-4. Downstream Temperature Distributions (°C) for Four Mile, Pen Branch, and Beaver Dam Creeks with Once-Through Towers for Each Reactor and for the Increased Pumping Alternative for D-Area[a]

	Month											
Location	Jan.	Feb.	March	April	May	June	July	Aug.	Sept.	Oct.	Nov.	Dec.
C-Reactor												
(Four Mile Creek)												
Discharge (1)[b]	19(28)	20(28)	23(28)	24(30)	26(30)	28(31)	29(32)	29(32)	28(31)	24(31)	23(29)	21(28)
Road A (2)	18(26)	18(26)	21(26)	23(28)	25(29)	28(30)	29(31)	29(31)	27(30)	23(29)	21(27)	19(26)
Road A-13 (3)	17(24)	17(24)	21(25)	23(28)	25(29)	28(30)	29(31)	28(31)	27(30)	23(28)	20(26)	18(25)
Swamp Delta (4)	15(22)	16(22)	19(23)	22(26)	25(28)	27(30)	28(30)	28(30)	26(29)	22(26)	19(24)	16(22)
Mouth (5)	13(20)	14(20)	18(21)	20(24)	23(27)	26(28)	27(29)	27(29)	25(27)	20(24)	17(21)	14(19)
Ambient Creek[c]	9(19)	11(19)	15(24)	19(25)	22(27)	25(31)	25(29)	25(29)	23(28)	21(25)	13(23)	13(18)
K-Reactor												
(Pen Branch)												
Discharge (6)	19(28)	20(28)	23(28)	24(30)	26(30)	28(31)	29(32)	29(32)	28(31)	24(31)	23(29)	21(28)
Road A (7)	18(27)	19(27)	22(27)	24(29)	26(30)	28(31)	29)32)	29(32)	28(31)	24(30)	22(28)	20(27)
RR Bridge (8)	18(26)	18(26)	21(26)	23(29)	26(30)	28(31)	29)31)	29(31)	28(30)	24(29)	21(27)	19(26)
Swamp Delta (9)	16(24)	17(24)	20(25)	23(27)	25(29)	28(30)	29(31)	28(31)	27(30)	23(28)	20(26)	18(24)
Above Steel Creek (10)	10(17)	12(17)	16(19)	18(21)	21(24)	24(26)	26(27)	25(27)	23(24)	18(21)	15(18)	11(16)
Mouth (11)	10(15)	12(16)	16(19)	18(20)	21(24)	24(26)	25(27)	25(26)	22(24)	17(21)	15(17)	11(15)
Ambient Creek[d]	8(18)	10(18)	15(22)	18(23)	21(24)	23(27)	23(27)	23(26)	21(26)	19(23)	13(21)	12(17)
D-Area[e]												
(Beaver Dam Creek)												
Discharge (12)	18(27)	16(22)	21(27)	24(29)	28(30)	29(32)	28(30)	28(31)	27(31)	27(32)	26(31)	19(31)
Swamp Delta (13)	17(25)	16(21)	20(26)	24(28)	27(30)	28(31)	28(30)	28(31)	27(30)	26(31)	24(29)	18(28)
Mouth (14)	13(20)	14(19)	17(21)	20(24)	24(27)	26(29)	27(29)	27(29)	25(27)	21(26)	19(23)	14(21)
Ambient creek[f]	8(15)	9(14)	12(17)	15(20)	19(22)	21(25)	23(27)	23(26)	23(26)	20(23)	17(22)	12(18)

a. Temperatures are monthly average - monthly extremes are in parentheses.
b. Corresponds to stream locations shown as squares on Figure B-2.
c. U.S. Geological Survey data for water year 1985 for station 02197342; Four Mile Creek at Road A-7 (USGS, 1986).
d. U.S. Geological Survey data for water year 1985 for station 02197341; Pen Branch at Road B (USGS, 1986).
e. Increased pumping alternative for D-Area. This alternative is equivalent to existing system for average conditions.
f. Average U.S. Geological Survey data for water years 1976-1985 for station 01297320; Savannah River near Jackson, S.C. (USGS; 1977, 1978, 1979, 1980, 1981, 1982, 1983, 1984, 1985, 1986).

BC-4
BC-14
BC-15

Table B-5. Downstream Temperature Distributions (°C) for Four Mile, Pen Branch, and Beaver Dam Creeks with Recirculating Towers for Each Reactor and for the Increased Pumping Alternative for D-Area[a]

Location	Month											
	Jan.	Feb.	March	April	May	June	July	Aug.	Sept.	Oct.	Nov.	Dec.
C-Reactor												
(Four Mile Creek)												
Discharge (1)[b]	14(25)	15(25)	18(26)	20(28)	23(28)	26(29)	27(30)	26(30)	25(29)	20(28)	18(27)	15(26)
Road A (2)	9(16)	11(16)	15(18)	18(21)	22(25)	25(27)	27(28)	26(28)	23(25)	17(21)	14(18)	10(15)
Road A-13 (3)	8(15)	11(16)	15(18)	18(21)	22(25)	25(28)	27(29)	26(28)	23(25)	17(21)	14(17)	9(15)
Swamp Delta (4)	8(15)	10(15)	14(17)	19(21)	22(26)	26(28)	27(29)	27(29)	24(26)	17(20)	13(16)	9(14)
Mouth (5)	7(14)	10(14)	14(17)	17(19)	20(23)	24(25)	25(26)	25(25)	21(23)	15(19)	13(15)	8(13)
Ambient Creek[c]	9(19)	11(19)	15(24)	19(25)	22(27)	25(31)	25(29)	25(29)	23(28)	21(25)	13(23)	13(18)
K-Reactor												
(Pen Branch)												
Discharge (6)	14(25)	15(25)	18(26)	20(28)	23(28)	26(29)	27(30)	26(30)	25(29)	20(28)	18(27)	15(26)
Road A (7)	11(19)	12(18)	16(20)	19(24)	23(27)	26(28)	27(29)	27(29)	24(27)	19(25)	15(21)	12(19)
RR Bridge (8)	9(17)	11(17)	15(19)	19(23)	23(26)	26(28)	27(29)	27(29)	24(27)	18(23)	15(19)	11(17)
Swamp Delta (9)	8(15)	11(16)	15(18)	19(22)	23(26)	26(28)	28(29)	27(29)	24(26)	17(21)	14(17)	9(15)
Above Steel Creek (10)	7(14)	10(14)	14(16)	15(17)	17(20)	21(23)	23(24)	22(23)	18(19)	13(17)	12(15)	8(12)
Mouth (11)	10(14)	11(15)	15(19)	18(20)	21(24)	25(26)	25(27)	23(24)	20(23)	13(19)	15(17)	11(14)
Ambient Creek[d]	8(18)	10(18)	15(22)	18(23)	21(24)	23(27)	23(27)	23(26)	21(26)	19(23)	13(21)	12(17)
D-Area[e]												
(Beaver Dam Creek)												
Discharge (12)	18(27)	16(22)	21(27)	24(29)	28(30)	29(32)	28(30)	28(31)	27(31)	27(32)	26(31)	19(31)
Swamp Delta (13)	17(25)	16(21)	20(26)	24(28)	27(30)	28(31)	28(30)	28(31)	27(30)	26(31)	24(29)	18(28)
Mouth (14)	15(22)	15(19)	18(23)	22(26)	26(28)	27(30)	27(29)	27(30)	26(29)	24(28)	22(26)	16(24)
Ambient creek[f]	8(15)	9(14)	12(17)	15(20)	19(22)	21(25)	23(27)	23(26)	23(26)	20(23)	17(22)	12(18)

a. Temperatures are monthly average - monthly extremes are in parentheses.
b. Corresponds to stream locations shown as squares on Figure B-2.
c. U.S. Geological Survey data for water year 1985 for station 02197342; Four Mile Creek at Road A-7 (USGS, 1986).
d. U.S. Geological Survey data for water year 1985 for station 02197341; Pen Branch at Road B (USGS, 1986).
e. Increased pumping alternative for D-Area. This alternative is equivalent to existing system for average conditions.
f. Average U.S. Geological Survey data for water years 1976-1985 for station 01297320; Savannah River near Jackson, S.C. (USGS; 1977, 1978, 1979, 1980, 1981, 1982, 1983, 1984, 1985, 1986).

BC-4
BC-14
BC-15

The existing system discharge flow is approximately 11 cubic meters per second and consists of heat exchanger effluent (at Savannah River temperature raised according to equation 2 of Section B.2.2) plus auxiliary flow (assumed to be at Savannah River temperature). The D-Area discharge flow is about 2.6 cubic BC-4 meters per second (up to 4.0 cubic meters per second during extreme conditions BC-14 for the increased pumping alternative); its temperature is equal to the BC-15 Savannah River temperature plus 8°C (plus 5°C during maximum flow conditions for the increased pumping alternative).

Tables B-3 and B-4 indicate the large, incremental change in stream temperatures from the existing system to the once-through towers. A further decrease in stream temperatures (as well as a large decrease in stream flow) occurs when recirculating towers are used (Table B-5). Downstream temperatures can increase when recirculating systems are used because the equilibrium temperatures (which the stream temperatures approach) are higher than those of the discharge while the flow is small. Downstream temperatures can increase because of both positive heat flux (into the water surface) and mixing with creek flow (other than reactor effluent).

The heat balance, and therefore the equilibrium temperature, takes into account spatial and temporal variations in vegetative cover of the streams. BC-4 Four Mile Creek and Pen Branch were broken down into three spatial regimes BC-14 [upper reach, middle reach, and lower (swamp) reach]; Beaver Dam Creek was considered to consist of an upper and lower reach. The percent of vegetative BC-15 shading was defined for each month of the year for each reach (Morris, 1987b). Values ranged from less than 10 percent in the winter (all reaches) to 90 percent in the swamp during the summer.

B.4 SAVANNAH RIVER DILUTION - D-AREA MODEL (SRDD)

B.4.1 MODEL DESCRIPTION

The dispersion of a source of water with a temperature (or concentration) elevated above that of the receiving water can be thought of as occurring in two steps. The "near field" is the area in the immediate vicinity of the discharge in which the mechanical mixing engendered by the difference in discharge and receiving water momentum dominates the dispersion process. After the discharge momentum has dissipated, the "far field" mechanism of receiving water turbulence causing mixing of the discharge and receiving waters is dominant. If the discharge momentum is relatively small (i.e., discharge velocity approximately equal to receiving water velocity), the near field can be (conservatively) neglected.

The far field dispersion of a steady nondecaying point source discharge into a current of velocity, u, can be described by (NRC, 1977):

TC

$$\frac{\partial uC}{\partial x} = \frac{\partial}{\partial y} K_y \frac{\partial C}{\partial y} + \frac{K_z}{\partial_z} \frac{\partial C}{\partial z} \qquad (16)$$

where C = temperature or concentration excess above ambient
u = ambient velocity, m/sec
x = downstream distance, m
y = lateral distance (i.e., perpendicular to current), m
z = depth, m
K_y, K_z = lateral and vertical diffusion coefficient, m^2/sec

Longitudinal diffusion is assumed to be negligible when compared with advection in the same direction. Also, temperature can be considered to be a non-decaying (i.e., no heat transfer to the atmosphere) source within the region of interest because the affected areas are small. In any case, omission of surface heat transfer is a conservative assumption.

Equation 16 states that the excess concentration is moved downstream by advection (movement by the current, left side of Equation 16) and laterally and vertically in the direction of decreasing concentration by turbulence (first and second term on right side of Equation 16, respectively). If u, K_y, and K_z are taken to be constants, then Equation 16 becomes:

$$u \frac{\partial C}{\partial x} = K_y \frac{\partial^2 C}{\partial y^2} + K_z \frac{\partial^2 C}{\partial z^2} \tag{17}$$

For an infinite receiving water, laterally and vertically surrounding the discharge point, the analytical solution to Equation 17 is:

$$\frac{C}{C_0} = \frac{Q}{4\pi \times \sqrt{K_y K_z}} \exp\left[\frac{-u(y_s - y)^2}{4K_y x}\right] \exp\left[\frac{-u(z_s - z)^2}{4K_z x}\right] \tag{18}$$

where C_o = excess temperature (or concentration) of the discharge
Q = discharge flow, m^3/sec
y_s = lateral distance of source from coordinate origin
z_s = vertical distance of source from coordinate origin

and the discharge is assumed at $x = 0$.

The Gaussian distribution of Equation 18 can be generalized for a receiving water of finite dimensions by adding images of the concentration distribution, Equation 18, from the bounding surfaces; that is, the infinite distribution of Equation 18 can be "folded" back into the water body at the boundaries, with the folded excess concentrations each being a component of the total excess concentrations. One can picture an infinite number of folds (e.g., the left-hand side of the lateral distribution would be folded at the left boundary; the resulting distribution would then laterally exceed the right boundary and would have to be folded there, etc.) for each side (of the source) for both the lateral (shorelines) and vertical (surface and bottom) directions (i.e., four infinite series). The mathematical description of these images or folds is (NRC, 1977):

$$\frac{C}{C_0} = \frac{Q}{4\pi \times \sqrt{K_y K_z}} f(y)\, f(z) \tag{19}$$

where:

$$f(w) = \sum_{m=-\infty}^{\infty} \exp\left[\frac{-u(2mW + w_s - w)^2}{4 K_w x}\right] + \sum_{m=-\infty}^{\infty} \exp\left[\frac{-u(2mW - w_s - w)^2}{4 K_w x}\right]$$

TC

and $w = y$ or z
$W = B$ (receiving water width) if $w = y$ or D (receiving water depth) if $w = z$

Note that $f(y)$ and $f(z)$ describe the infinite folds of the first and second exponential terms, respectively, of Equation 18.

A further refinement of the analysis stems from the assumption of a point source discharge. Equation 19 can be generalized to account for an arbitrary discharge geometry by integrating over the discharge dimensions (i.e., consider the discharge an infinite number of point sources), where Q would then be the discharge flow per unit discharge size (i.e., length for a line source or area for a plane source). Such an integration of Equation 19 would have to be performed numerically and would be very time-consuming, computationally. Accordingly, an analytical approximation to this integration has been used.

The areal nature of the discharge source is accounted for by taking a virtual source distance x_v; x_v corresponds to the distance, x, at which (for $y = y_s$ and $z = z_s$) C/C_o equals 1 in Equation 19. Accordingly, Equation 19 is modified by replacing x with $x + x_v$. The use of a virtual source distance assures conservation of mass, avoids the mathematical singularity at $x = 0$, and ensures that the calculated concentration (or temperature) at the source is equal to that being discharged.

B.4.2 MODEL USE

The model described in Section B.4.1 was generalized for use in calculating the temperature distribution in the Savannah River from the multiple-source D-Area sparge discharge system. Based on preliminary design assumptions, the system would consist of approximately 65 discharge pipes, 20 centimeters in diameter and 9 meters long, spaced at 3-meter intervals and aligned along the river bank. SRDD models such a system by considering each of the discharge pipes as a component to the overall temperature (or concentration) distribution. Distances x are measured, for each pipe, from that pipe ($x = 0$ is taken at the upstream pipe). Virtual source distances, x_v, are calculated individually for each pipe (i.e., C/C_o equals 1 at each pipe, accounting for the contributions of all upstream sources).

The total discharge flow is 2.6 cubic meters per second, 0.04 cubic meter per second per discharge pipe; the discharge water velocity is 1.2 meters per second, and its excess temperature is 8°C (above the temperature of the river). Table B-6 lists the Savannah River parameters used in the analysis. The approximate river cross-section at the discharge (average width = 61 meters, average depth = 3.2 meters) was known for a base river flow of 188 cubic meters per second. Log-log interpolations of river gage heights at Jackson for this flow (gage height = 2.28) and for 490 cubic meters per second [gage height = 4.62 meters (USGS, 1981)] were performed for the seasonal

Table B-6. Savannah River Parameters Used in Analysis

Parameter	Winter average	Spring average	Summer average	Summer extreme
Flow (m^3/sec)	345.0	371.0	212.0	159.0
Width (m)	70.0	71.0	65.0	59.0
Depth (m)	4.6	4.8	3.5	2.9
Temperature (°C)	8.0	17.0	23.0	28.0
Horizontal diffusion coefficient (m^2/sec)	.26	.26	.26	.26
Vertical diffusion coefficient (m^2/sec)	.0026	.0026	.0026	.0026

flows. The change in gage height between the interpolated value and that at the base flow was assumed to be the change in average depth at the discharge. Typically, as the flow increases, the width, depth, and velocity of the river increases. Average widths were assumed to be the mean of 61 meters (known width at the base flow) and that width that would result in the same average river velocity as that at the base flow. These assumptions will result in river dimensions that accede to the typical river dimension-flow characteristics described above.

For the region near the discharge (about 100 meters from the discharge), the temperature distribution will be (for a given velocity) insensitive to the river dimensions. This occurs because the plume has not had time to grow sufficiently such that the images from the far boundaries (Georgia shoreline and river bottom) are important. In addition, the temperature at any given coordinate decreases with increasing river velocity. This is apparent from Equation 19, which shows that the river velocity, u, enters the temperature function as exp(-u).

The chosen horizontal diffusion coefficient is based on studies of the Savannah River approximately 20 kilometers downstream (Steel Creek) from the discharge (Du Pont, 1981, Appendix A). The vertical diffusion coefficient is typically one to two orders of magnitude smaller than the horizontal diffusion coefficient (NRC, 1977; Yotsukura and Sayre, 1976; Fischer, 1969). Calculations with K_z = 0.0026 and 0.026 square meter per second indicate that the former yields larger values of maximum isotherm width and cross-sectional area. However, at distances farther downstream than considered here, the discharge will be fully mixed vertically and the distribution will be independent of K_z. K_z = 0.0026 square meter per second was used in the analysis.

B.4.3 MODEL RESULTS

Table B-7 lists the river withdrawal and discharge temperatures along with the
zones of passage for each seasonal case. The discharge temperatures for this BC-4
alternative, unlike the others, are based on elevating measured Savannah River BC-14
temperatures (rather than being measured discharge temperatures). This is BC-15

Table B-7. Temperatures and Zone of Passage Sizes for D-Area Coal-fired Powerhouse Direct Discharge into Savannah River

Parameter	Winter average	Spring average	Summer average	Summer extreme
Temperature (°C)				
Withdrawal from river	8.0	17.0	23.0	28.0
Discharge	16.0	25.0	31.0	36.0
Maximum river cross-sectional area (percent of total) having temperature (°C) less than				
2.8 (excess)	99.7	99.7	99.5	99.3
32.2 (absolute)	100	100	100	99.7
Maximum river width (percent of total) having temperature excess (°C) less than				
2.8 (excess)	95	95	94	93
32.2 (absolute)	100	100	100	96

BC-4 because comparison between river and discharge are relevant and need to be on
BC-14 the same basis. The extreme summer conditions result in the smallest zones of
BC-15 passage. Figure B-3 shows the maximum cross-sectional area (as a fraction of the total), and downstream extent (meters from the discharge pipe farthest upstream) as a function of excess temperature for extreme summer conditions. Excess temperatures corresponding to those extents less than 3 meters downstream from the discharge pipe located farthest downstream will actually exist intermittently in the river; that is, such isopleths (greater than 2.8°C) exist near each discharge pipe but will dissipate between pipes.

Figure B-3 also shows the suggested width and cross-sectional area of the zone of passage. This figure shows that the direct discharge will be well within the suggested zone-of-passage criteria.

B.5 FOG MODEL

The occurrences of ground-level fogging, icing, elevated visible plumes, and ground deposition rates of dissolved solids in drift in the environmental impact statement were calculated by the NUS computer code FOG (Fisher, 1974). The FOG model provides predictions of these environmental impacts over a geographical area surrounding the site. For these analyses, sequential hourly meteorological data representative of the geographical areas surrounding C-Area and K-Area at the Savannah River Plant were used for the 5-year period from January 1975 to October 1979.

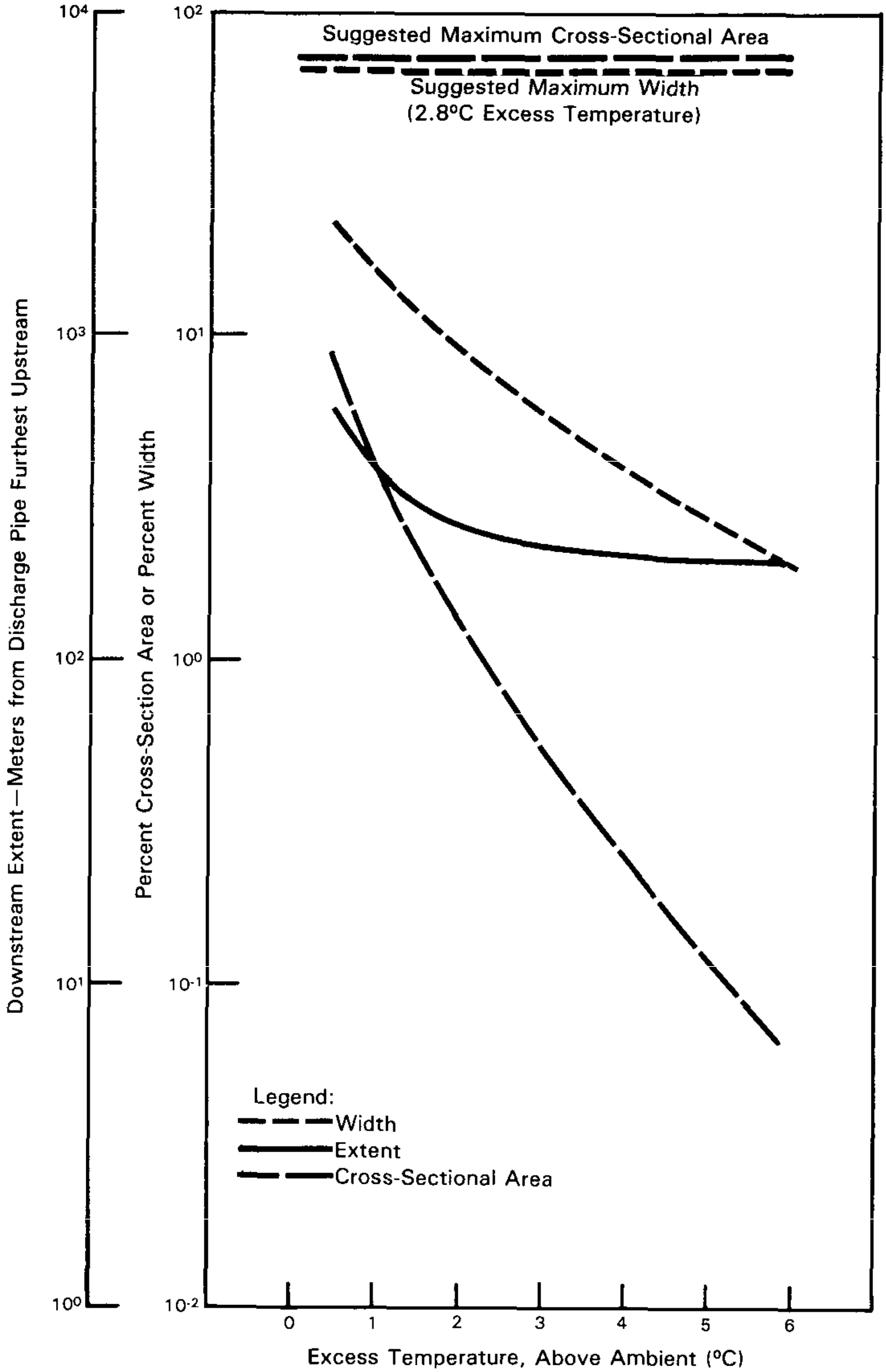

Figure B-3. Extreme Summer Plume Characteristics

The FOG model simulates the dispersion of a plume from evaporative cooling systems using sequential meteorological data. It defines a bent-over plume using the Briggs plume rise equations (Briggs, 1969) out to the distance at which the plume levels off, and Gaussian dispersion equations at greater distances. The plume buoyancy employed in the calculations is computed from the effluent temperature and airflow rate at the exit of the cooling tower and from the ambient dry-bulb temperature and relative humidity. The merging of plumes from the round, mechanical-draft, multifan cooling towers is considered using equations developed by Briggs (1974) for a cluster of cells.

The plume is assumed to propagate rectilinearly, and any meandering effects due to wind shifts are neglected. Atmospheric stability classes are those calculated from the standard deviation of wind direction fluctuations or, if these data are unavailable, from those reported by the National Weather Service for every hour for the period under consideration. The dispersion parameters used were those of Pasquill-Gifford (DOE, 1984c). Formulations for critical wind speed relative to the aerodynamic downwash of the exhaust plumes, in the wake of the tower under high wind conditions, are also included in the FOG model.

In addition to the preliminary design information contained in Chapter 2, the following assumptions were made in the analysis of fogging, icing, visible plumes, and ground deposition rates of dissolved solids:

- Circulating water flow = 11.3 cubic meters per second
- Drift rate (percent of circulating water flow) = 0.006 percent
- Total dissolved solids concentrations (TDS) in influent water = 53 parts per million
- Cycles of concentration for recirculating towers = 3
- Drift droplet size (mass median diameter) = 376 microns
- Air flow rate for mechanical draft recirculating tower = 13,848 cubic meters per second

B.5.1 INDUCED GROUND-LEVEL FOGGING

For the purposes of these analyses, induced ground-level fog is defined as a reduction in ground-level visibility to 1000 meters or less as a result of the operation of the cooling system. Huschke (1959) defines the 1000-meter distance as the limit on visibility above which fog is not considered to occur. The water content of the plume at ground level is calculated by means of the Gaussian dispersion analysis discussed above; all moisture in excess of that required to saturate the ambient air is assumed to form condensed water droplets. An empirical equation (Pettersen, 1956) is then used to relate the atmospheric water content to the horizontal visibility.

B.5.2 INDUCED GROUND-LEVEL ICING

The frequencies of occurrence of various ice thicknesses resulting from the operation of the cooling towers were also calculated by FOG code subroutines that simulate the formation and accumulation of ice and calculate the frequencies of ice occurrences.

The ice-formation routines predict accumulations of ice around a cooling system from the impingement of condensed water and drift droplets. Calculations of ice buildup are made for horizontal flat surfaces (e.g., roads). The rate of ice buildup can be limited either by the liquid water delivery rate to the collecting surface or by the heat balance necessary to sustain freezing conditions.

The dispersion of the relatively small condensed water droplets is treated the same as that of the vapor plume (i.e., by diffusion), while the transport of the drift droplets follows the ballistic trajectory method employed for the salt deposition calculations. The FOG model performs an energy balance on the surface or volume of interest. Ice formation is assumed to occur only when the ambient temperature is less than 0°C. Ice buildup on horizontal ground-level surfaces is assumed to result only from fallout of the drift droplets. Because the much smaller condensed water droplets have negligibly small settling velocities, the condensed water droplets are assumed not to impinge on flat horizontal surfaces. Melting due to solar radiation is included in the simulation for flat surfaces.

B.5.3 ELEVATED VISIBLE PLUMES

The FOG code was also used to calculate the frequencies of occurrence of elevated visible plumes over each grid point under consideration. The total flux of air through a cross-section of the plume normal to the plume axis is calculated at successive downwind distances. The amount of entrained air is computed as the difference between the total air flow and the air flow leaving the cooling system. The entrained air and effluent air from the cooling system are assumed to be thoroughly mixed isobarically and thermodynamic properties of the resulting mixture are calculated. A visible plume is predicted to occur at a particular point if calculations show that the mixed plume is supersaturated.

B.5.4 DRIFT DEPOSITION

Drift deposition analysis by the FOG code involves the following three calculations: (1) the sequential release of the entrained drift droplets from the effluent plume; (2) the subsequent horizontal transport of the drift droplets; and (3) the deposition rates at prespecified downwind distances for each wind direction.

It is assumed in the FOG model that the initial concentration of drift droplets follows a Gaussian distribution normal to the plume axis. The release of the entrained droplets at any point within the plume depends on the relative magnitudes of the terminal fall velocity of the droplets and the vertical velocity of the air in the plume. At each downwind distance under consideration, these two velocities are compared for each of the various size categories of drift droplets, and a fraction of the droplets released. This process is repeated until all drift droplets are released from the plume. This drift is carried by the ambient wind until it is deposited on the ground. The rate of fall of the drift droplets depends on the droplet size, which is changed by evaporation processes. These, in turn, depend on the physical and transport properties of both the liquid droplets and the surrounding air. A stepwise procedure is employed in the FOG code to compute the trajectory of the droplets by considering these transport, evaporation, and settling rate effects.

REFERENCES

Bird, R. B., W. E. Stewart, and E. N. Lightfoot, 1966. Transport Phenomena, John Wiley and Sons, Inc., New York City, New York.

Briggs, G. A., 1969. Plume Rise, TID-25075, Atomic Energy Commission Critical Review Series.

Briggs, G. A., 1974. Plume Rise from Multiple Sources, Cooling Tower Environment, Conference 740302, Symposium Proceedings at University of Maryland.

Codell, R., and W. K. Nuttle, 1980. Analysis of Ultimate Heat Sink Cooling Pond, U.S. Nuclear Regulatory Commission, NUREG-0693.

Dickey, J. B., Jr., and R. E. Cates, 1973. Managing Waste Heat with the Water Cooling Tower, 2nd edition, The Morley Company, Mission, Kansas.

DOE (U.S. Department of Energy), 1984a. Final Environmental Impact Statement, L-Reactor Operation, Savannah River Plant, Aiken, South Carolina, DOE/EIS-0108, Savannah River Operations Office, Aiken, South Carolina.

DOE (U.S. Department of Energy), 1984b. Thermal Mitigation Study, Compliance with the Federal and South Carolina Water Quality Standards, Savannah River Plant, Aiken, South Carolina, DOE/SR-5003, Savannah River Operations Office, Aiken, South Carolina.

DOE (U.S. Department of Energy), 1984c. Atmospheric Science and Power Production, DOE/TIC-27601, Washington, D.C.

Du Pont (E. I. du Pont de Nemours and Company), 1981. Savannah River Plant NPDES Permit Applications for System Permit Number SC0000175, compiled for the U.S. Department of Energy, Savannah River Operations Office, Aiken, South Carolina.

Edinger, J. R., and J. C. Geyer, 1965. Heat Exchange in the Environment, RP-49, Edison Electric Institute, Washington, D.C.

Firstenberg, H., and G. E. Fisher, 1976. An Investigation of Cooling Lakes for the Closed-Cycle Operation of Electric Generating Stations, Volume I, NUS Corporation, Gaithersburg, Maryland.

Fischer, H. B., 1969. "The Effect of Bends on Dispersion in Streams," Water Resources Research, Vol. 5, No. 2.

Fisher, G. E., 1974. FOG Model Description, NUS-TM-S-185, NUS Corporation, Gaithersburg, Maryland.

Harleman, D. R. F., 1972. "Longitudinal Temperature Distributions in Rivers and Estuaries," in Engineering Aspects of Heat Disposal from Power Generation, R. M. Parsons Laboratory for Water Resources and Hydrodynamics, Massachusetts Institute of Technology, Cambridge, Massachusetts, Chapter 6.

Huschke, R. E., 1959. Glossary of Meteorology, American Meteorological Society, Boston, Massachusetts.

Jacobsen, W. R., R. J. Brown, E. W. Rabon, and L. J. Tilly, 1972. Thermal Discharges from the Savannah River Plant, DPST-72-428, E. I. du Pont de Nemours and Company, Savannah River Laboratory, Aiken, South Carolina.

Morris, O. M. (Superintendent, NEPA Activities Department), E. I. Du Pont de Nemours and Company, Savannah River Laboratory, Aiken, South Carolina, 1987a. Letter dated March 4, 1987, RE: ACWS EIS-Transmittal #16 to W. E. Wisenbaker, Chief, Environmental Programs Branch, Environmental Division, U.S. Department of Energy, Savannah River Operations Office, Aiken, South
BC-4 Carolina.

BC-14
BC-15 Morris, O. M. (Superintendent, NEPA Activities Department), E. I. Du Pont de Nemours and Company, Savannah River Laboratory, Aiken, South Carolina, 1987b. Letter dated March 24, 1987, RE: ACWS EIS-Transmittal #17 to W. E. Wisenbaker, Chief, Environmental Programs Branch, Environmental Division, U.S. Department of Energy, Savannah River Operations Office, Aiken, South Carolina.

NCDC (National Climatic Data Center), 1983. Computer tape, Asheville, North Carolina.

Neill, J. S., and D. F. Babcock, 1971. The Dissipation of Reactor Heat at the Savannah River Plant, DP-1274, E. I. du Pont de Nemours and Company, Savannah River Laboratory, Aiken, South Carolina.

NRC (U.S. Nuclear Regulatory Commission), 1977. Estimating Aquatic Dispersion of Effluents from Accidental and Routine Reactor Releases for the Purpose of Implementing Appendix I, Regulatory Guide 1.113, Revision 1.

NUS Corporation, 1984. Feasibility Study: Savannah River Plant Cooling Water Alternatives, Savannah River Center, Aiken, South Carolina.

Perry, R. H. (editor), 1963. Chemical Engineers' Handbook, 4th edition, McGraw-Hill Book Company, New York City, New York.

Pettersen, S., 1956. Weather Analysis and Forecasting, Volumes I and II, McGraw-Hill, New York City, New York.

Ryan, P. J., 1972. "Temperature Prediction and Design of Cooling Ponds," in Engineering Aspects of Health Disposal From Power Generation, R. M. Parsons Laboratory for Water Resources and Hydrodynamics, Massachusetts Institute of Technology, Cambridge, Massachusetts.

Ryan, P. J., and K. D. Stolzenbach, 1972. "Environmental Heat Transfer," in Engineering Aspects of Heat Disposal from Power Generation, R. M. Parsons Laboratory for Water Resources and Hydrodynamics, Massachusetts Institute of Technology, Cambridge, Massachusetts.

Thackston, E. L., and F. L. Parker, 1971. Effect of Geographical Location on Cooling Pond Requirements and Performance, 16130FDQ, Water Pollution Control Research Series, Water Quality Office, U.S. Environmental Protection Agency.

USGS (U.S. Geological Survey), 1977. Water Resources Data, South Carolina, Water Year 1976, USGS/WRD/HD-77/001, Water Resources Division, Columbia, South Carolina.

USGS (U.S. Geological Survey), 1978. Water Resources Data, South Carolina, Water Year 1977, USGS/WRD/HD-78/003, Water Resources Division, Columbia, South Carolina.

USGS (U.S. Geological Survey), 1979. Water Resources Data, South Carolina, Water Year 1978, USGS/WRD/HD-79/004, Water Resources Division, Columbia, South Carolina.

USGS (U.S. Geological Survey), 1980. Water Resources Data, South Carolina, Water Year 1979, USGS/WRD/HD-80/051, Water Resources Division, Columbia, South Carolina.

USGS (U.S. Geological Survey), 1981. Water Resources Data, South Carolina, Water Year 1980, USGS/WRD/HD-80/66, Water Resources Division, Columbia, South Carolina.

USGS (U.S. Geological Survey), 1982. Water Resources Data, South Carolina, Water Year 1981, USGS/WRD/HD-81/046, Water Resources Division, Columbia, South Carolina.

USGS (U.S. Geological Survey), 1983. Water Resources Data, South Carolina, Water Year 1982, USGS/WRD/HD-82/078, Water Resources Division, Columbia, South Carolina.

USGS (U.S. Geological Survey), 1984. Water Resources Data, South Carolina, Water Year 1983, USGS/WRD/HD-85/208, Water Resources Division, Columbia, South Carolina.

USGS (U.S. Geological Survey), 1985. Water Resources Data, South Carolina, Water Year 1984, USGS/WRD/HD-86/214, Water Resources Division, Columbia, South Carolina.

USGS (U.S. Geological Survey), 1986. Water Resources Data, South Carolina, Water Year 1985, USGS/WRD/HD-87/213, Water Resources Division, Columbia, South Carolina.

Yotsukura, N., and W. W. Sayre, 1976. "Transverse Mixing in Natural Channels," Water Resources Research, Vol. 12, No. 4.